Tunneling spectroscopic study of finite superlattices

R. J. Aggarwal,[a] M. A. Reed,[b] W. R. Frensley,[c] Y.-C. Kao, and J. H. Luscombe
Central Research Laboratories, Texas Instruments Incorporated, Dallas, Texas 75265

(Received 15 February 1990; accepted for publication 20 June 1990)

We present a tunneling density of states study of the transition from a superlattice miniband to a sequential coupled well structure. We have observed by tunneling spectroscopy the eigenstates of a finite superlattice system far below the Stark localization threshold. The transition from an indistinguishable miniband to a coupled well structure is experimentally found to be 2.5 meV $\leqslant W$(miniband width)$/n$(# periods) $\leqslant$10.5 meV.

Semiconductor superlattices have received renewed interest for the design and fabrication of novel electronic structures utilizing perpendicular transport. A central issue for the design, utilization, and analysis of superlattice structures is the nature of the electronic states. In weakly coupled superlattices it has been shown[1] that the perpendicular transport proceeds via sequential tunneling, whereas under the proper conditions a miniband forms.[2–4] We present here a tunneling density of states study of the transition of a finite superlattice from a superlattice miniband to a coupled well structure.

A generic superlattice tunnel diode structure[5] was utilized to study the density of states in a series of superlattices. Figure 1 shows a self-consistent band diagram at resonant bias (a), along with the experimental current (I) [and conductance (G)] versus voltage (V) characteristics (b), of the type of structures investigated in this study. This specific example is a structure identical to the initial work of Davies *et al.*[5] The band diagram is determined from a self-consistant finite temperature Thomas–Fermi zero-current calculation,[6] with the superlattice structure determined from an envelope function calculation superimposed. When the top of the first collector miniband crosses the bottom of the available emitter electron supply, a decrease in current occurs due to the requirement to conserve both energy and momentum. This is defined as the resonant (peak) voltage. It should be emphasized that realistic band diagrams are necessary for an accurate understanding of resonant effect.

Table I illustrates the series of superlattice structures investigated. Structure S1 was identical to that of Davies *et al.*[5] The remaining samples consisted of a Cr-doped semi-insulating GaAs substrate, a 0.5 μm undoped GaAs buffer, a 1.0 μm 1×10^{18} cm^{-3} n^+-GaAs bottom contact, a 420 Å 1×10^{17} cm^{-3} (last 20 Å undoped) GaAs contact to superlattice transition region, a superlattice/tunnel barrier/superlattice region symmetric about the tunnel barrier, a 400 Å 2×10^{18} cm^{-3} GaAs top contact, and an InGaAs top nonalloyed ohmic contact. To study the effects of contact doping, S3 had symmetric 400 Å 1×10^{17} cm^{-3} contact regions adjacent to the superlattices. S5 was identical to S4, except that the bottom superlattice was replaced with bulk GaAs (though the doping modulation was identical). Structural parameters were verified by cross-section transmission electron microscopy, and photoluminescence of nominally identical superlattices (grown without doping and contact structures) was used to verify superlattice

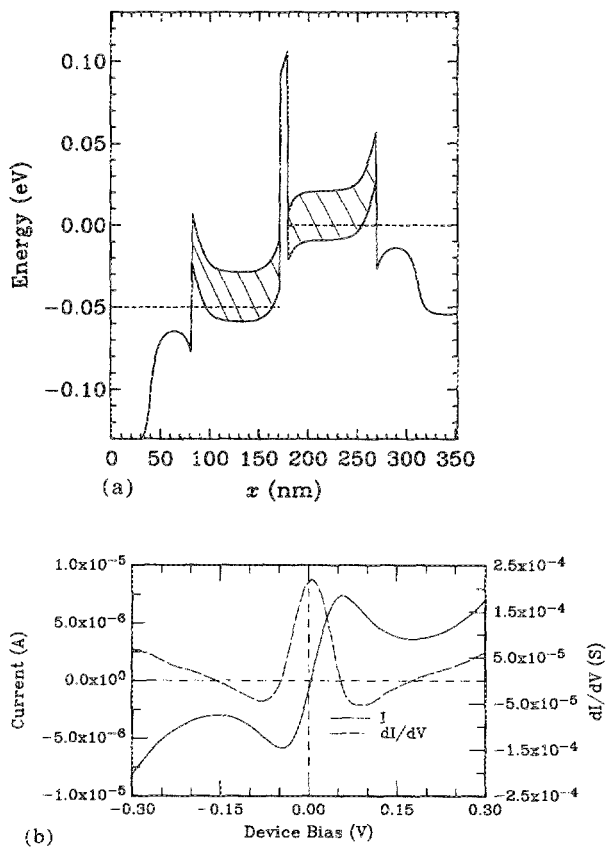

FIG. 1. (a) Self-consistent Γ-point energy band vs epitaxial dimension of sample S1 at resonant bias. The hatched regions denote the 25-meV-wide lowest superlattice minibands and the dotted lines the Fermi level. The structure is identical to that reported by Davies *et al.* (Ref. 15) $T=4.2$ K. (b) Experimental current (solid) and conductance (dashed) vs voltage characteristics of S1. $T=4.2$ K.

[a]Department of Electrical Engineering and Computer Science, Massachusetts Institute of Technology, Cambridge, MA 02139.
[b]New address: Department of Electrical Engineering, Yale University, P. O. Box 2157 Yale Station, New Haven, CT 06520-2157.
[c]New address: Erik Jonsson School of Electrical Engineering and Computer Science, University of Texas at Dallas, P. O. Box 830688, Richardson, TX 75083-0688.

 0003-6951/90/330707-03$02.00

TABLE I. Summary of the superlattice tunneling structures investigated. $E_{SL,min} - E_c$ denotes the energy of the bottom of the first miniband (in meV), referenced to GaAs. W denotes the width (in meV) of the first miniband. The superlattice minibands were calculated using an infinite envelope function approximation. $E_{F,SL} - E_c$ denotes the Fermi energy of the superlattice (in meV), referenced to GaAs.

Sample	d_{GaAs}/d_{AlGaAs} (Å)	$E_{SL,min} - E_c$ (meV)	W (meV)	$E_{F,SL} - E_c$ (MeV)
S1	60/30	53	30	62
S2	40/50	90	25	96
S3	49/14	45	105	57
S4	40/10	43	190	55
S5	40/10 (asymmetric)	43	190	55

band gap and aluminum content. Mesas as small as $4(\mu m)^2$ were fabricated using standard contact lithography processing.

The superlattice structure S1 is presented to compare to previous work.[5] Structures S2–4 are also ten period superlattices, designed such that the superlattice miniband widths span the available range in the conduction band. The GaAs wells of these superlattices were doped at 1×10^{17} cm^{-3}, the $Al_{0.23}Ga_{0.77}As$ barriers were nominally undoped, and the tunneling barrier was kept fixed at 100 Å of $Al_{0.23}Ga_{0.77}As$. S2 has the same approximate miniband width as S1, with the second miniband "virtual" only. S3 is designed to have the same approximate superlattice energy centroid as S2, with a factor of 4 larger miniband width. S3 and S4 have the same miniband minimum, with S4 having almost a factor of 2 larger miniband width than S3. In addition, the top of S4's first miniband is "virtual." S5's superlattice is identical to S4, except the asymmetry allows one to investigate injection into a superlattice from a 3D system, and vice versa.

The superlattice Fermi levels were calculated by assuming free electrons in the transverse directions and Bloch states for the vertical direction. The Fermi level was then inferred as the chemical potential which leads to a miniband-occupied carrier density corresponding to the average carrier concentration of the sample.[7] It should be noted that determination of the superlattice Fermi level in general produces a higher Fermi level than that for a bulk system of the same density.

The I-V and G-V characteristics of samples S1 and S2 are very similar, exhibiting well-defined negative differential resistance (NDR) at low temperature [with peak-to-valley (P/V) current ratios as high as 2:1 for S1, 2.4:1 for S2]. NDR is observable (P/V 1.3:1) at room temperature in S2, and an inflection is clearly evident at room temperature in S1.[8] Aside from the major resonance (Fig. 1), there is no apparent additional structure in the conductance greater than the 1 mV (i.e., 12 K) experimental resolution for either S1 or S2, at a sample temperature of 4.2 K (immersed).

We now experimentally increase the superlattice miniband from 25 to 105 meV and examine the vertical transport. Figure 2 shows the low-voltage I-V and G-V characteristics of S3 at 4.2 K. The $\pm\sim120$ mV major peak

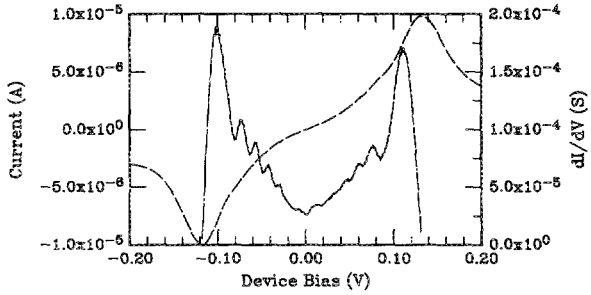

FIG. 2. Low-voltage I-V (solid) and G-V (dashed) characteristics of sample S3 (105-meV-wide superlattice miniband) at 4.2 K. The $\pm\sim120$ mV major resonances corresponds to the alignment line-up of the first minigap with the emitter.

corresponds to the line-up of the first minigap with the emitter. A series of peaks on the low bias side of the major peak is apparent. Note that these biases correspond to electric fields well below that expected for Stark localization.[9,10] The condition for Stark localization of a superlattice is $eEd > W$, where E is the applied electric field, d is the superlattice period, and W the width of the miniband under consideration. At the biases considered here, the Stark splitting is < 10 meV, compared to a miniband width of 105 meV. The "subresonant series" starts to degrade above 20 K, and is unobservable (except for the highest subresonance peak) above 50 K.

Figure 3 shows the I-V and G-V characteristics of a superlattice miniband experimentally increased to 190 meV (S4), keeping the number of superlattice periods constant. The subresonance series is very pronounced; higher bias peaks are evident even at room temperature. Assuming that the structure is due to the finite extent of the superlattice, we calculate the single electron transmission coefficient of the ten-period superlattice/coupled quantum well system, and map these ten resonant peaks onto the self-consistent band structure. Figure 4 shows the calculated resonant crossings of the collector finite superlattice transmission peaks with the emitter Fermi level, compared with the experimental resonant peaks. The calibration of the top resonance is determined by the number of periods in the finite superlattice, and the low peak cutoff is determined from the superlattice Fermi level. The agreement between calculated and experimental peak position is qualitatively (a $V^{1/2}$ behavior) and quantitatively good. Like-

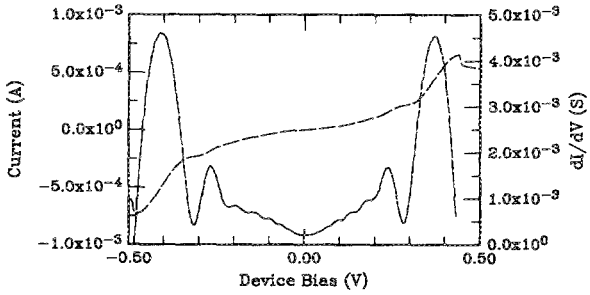

FIG. 3. Low-voltage I-V (dashed) and G-V (solid) characteristics of sample S4 (190-meV-wide superlattice miniband) at 10 K.

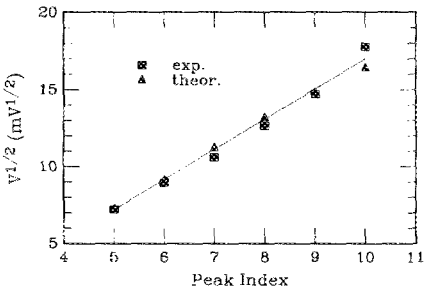

FIG. 4. Experimental (square) and theoretical (circle) resonant crossings of the collector finite superlattice transmission peaks with the emitter superlattice Fermi level. The calculated resonant crossings were determined from mapping the finite superlattice transmission peaks onto the self-consistent band structure and determining the bias at which they cross the emitter Fermi level.

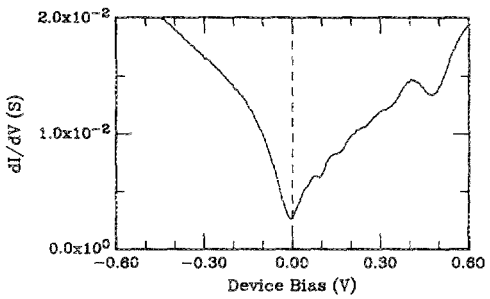

FIG. 5. *G-V* characteristics of sample S5 (S4 with one superlattice replaced with bulk GaAs). $T = 10$ K. Positive bias corresponds to electron injection from the bulk GaAs into the finite superlattice.

wise, S3 shows similarly good agreement.[8] High-voltage deviation may indicate a zero-current model is no longer valid.

The absence of structure in S1 and S2 implies that we have experimentally observed the transition (in this system) from an indistinguishable miniband to a coupled-well structure. In energy, this implies the transition occurs between state splittings of 4 meV (the maximum in S1) and 8 meV (the minimum observable in S3), when $kT <$ the state splitting $E(i+1) - E(i)$. Note that this is a function of the position of eigenstate i within the miniband. In rationalized units, this corresponds to 2.5 meV $< W$(miniband width)$/n$(# periods) $<$ 10.5 meV. The origin of the eigenstate broadening mechanism (such as epitaxial or alloy fluctuations) is not known.

To check that the resonances are indeed arising from the collector density of states, a sample (S5) identical to S4 but with bulk GaAs on one side of the superlattice was investigated. Figure 5 shows the *G-V* characteristics of this structure at 10 K. Positive bias corresponds to electron injection from the bulk GaAs into the finite superlattice. Under this condition, the position and number of the subresonance peaks compares well with that of the finite superlattice injector sample. As has been pointed out earlier,[11] there is no structure in the reverse bias direction since the collector is bulk. It should be noted that the lower Fermi level in the bulk GaAs (versus the replaced superlattice) accounts for the voltage shift of the subresonant peaks.

In summary, we have observed by vertical tunneling transport the eigenstates of a finite superlattice system far below the Stark localization threshold.

We are thankful to R. T. Bate, D. C. Collins, and C. Fonstad for constant support and encouragement, to W. M. Duncan for the photoluminescence measurements, to J. N. Randall for discussions, to H.-L. Tsai for cross-section TEMs, and to R. K. Aldert, P. Q. Montague, E. D. Pijan, P. F. Stickney, F. H. Stovall, and J. R. Thomason for technical assistance. This work was done under the MIT-TI VI-A Internship Program, and was supported in part by the Office of Naval Research.

[1] K. K. Choi, B. F. Levine, R. J. Malik, J. Walker, and C. G. Bethea, Phys. Rev. B **35**, 4172 (1987).
[2] T. Dufficld, R. Bhat, M. Koza, F. DeRosa, D. M. Hwang, P. Grabbe, and S. J. Allen, Jr., Phys. Rev, Lett. **56**, 2724 (1986).
[3] B. Deveaud, J. Shah, T. C. Damen, B. Lambert, and A. Regeny,Phys. Rev. Lett. **58**, 2582 (1987).
[4] A. Sibille, J. F. Palmier, H. Wang, and F. Mollot, Phys. Rev. Lett. **64**, 52 (1990).
[5] R. A. Davies, M. J. Kelly, and T. M. Kerr, Phys. Rev. Lett. **55**, 1114 (1985).
[6] M. A. Reed, W. R. Frensley, W. M. Duncan, R. J. Matyi, A. C. Seabaugh, and H.-L. Tsai, Appl. Phys. Lett. **54**, 1256 (1989).
[7] J. H. Luscombe, R. J. Aggarwal, M. A. Reed, W. R. Frensley, and M. Luban (unpublished).
[8] The temperature dependence of S2 is nontrivial due to the screening of the superlattice contacts. A full discussion of the transport, characterization, and analysis of structures S1-S4 can be found in R. J. Aggarwal, Master's thesis, MIT, 1990.
[9] R. F. Kazarinov and R. A. Suris, Fiz. Tekh. Poluprov. **5**, 797 (1971) [Sov. Phys. Semicond. **5**, 707 (1971)].
[10] L. L. Chang, L. Esaki, A. Segmüller, and R. Tsu, in *Proceedings of the Twelfth International Conference on the Physics of Semiconductors*, edited by M. H. Pilkuhn (B. G. Teubner, Stuttgart, 1974), p. 688.
[11] P. England, J. R. Hayes, J. P. Harbison, D. M. Hwang, and L. T. Florez, Appl. Phys. Lett. **53**, 391 (1988).